Electronic Supplementary Material (ESI) for Dalton Transactions.

Supporting Information

Synthesis of tris(3-pyridyl)aluminate ligand and its unexpected stability against hydrolysis: revealing cooperativity effects in heterobimetallic pyridyl aluminates

Álvaro García-Romero,[a] Jose M. Martín-Álvarez,[a] Annie L. Colebatch,[b,c] Alex J. Plajer,[d] Daniel Miguel,[a] Celedonio M. Álvarez, [a]* and Raúl García-Rodríguez [a]*

[a] *GIR MIOMeT-IU Cinquima-Química Inorgánica Facultad de Ciencias, Universidad de Valladolid; Campus Miguel Delibes, 47011 Valladolid (Spain). E-mail: celedonio.alvarez@uva.es , raul.garcia.rodriguez@uva.es*
[b] *Chemistry Department. Cambridge University, Lensfield Road, Cambridge CB2 1EW (U.K.)*
[c] *Research School of Chemistry. Australian National University Canberra, ACT, 2601 (Australia)*
[d] *Chemical Research Laboratory 12 Mansfield Road, Oxford, OX1 3TA (UK)*

Contents

NMR studies, NMR spectra and high-resolution mass spectrometry data of 1Li

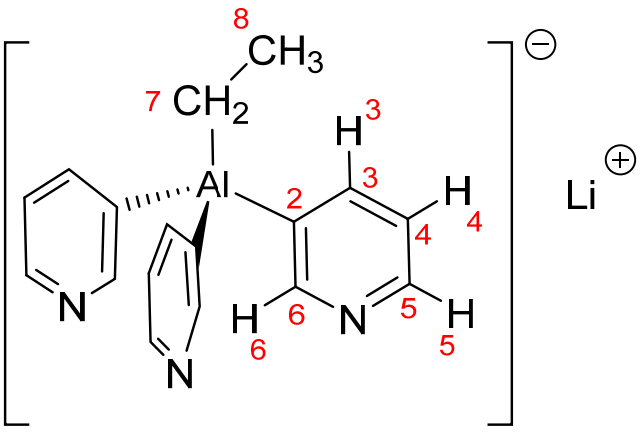

*Figure S1. Compound **1**Li, [EtAl(3-py)$_3$]Li, with the atom labelling used in the NMR studies.*

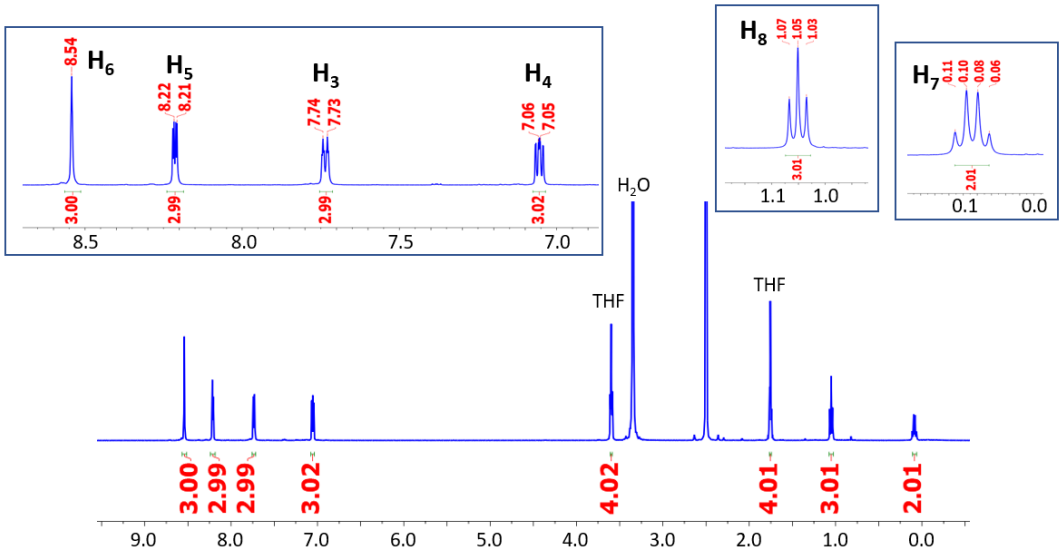

*Figure S2. ^{1}H NMR (298 K, DMSO-d_6, 500 MHz) spectrum of **1**Li ([EtAl(py)$_3$]Li·THF).*

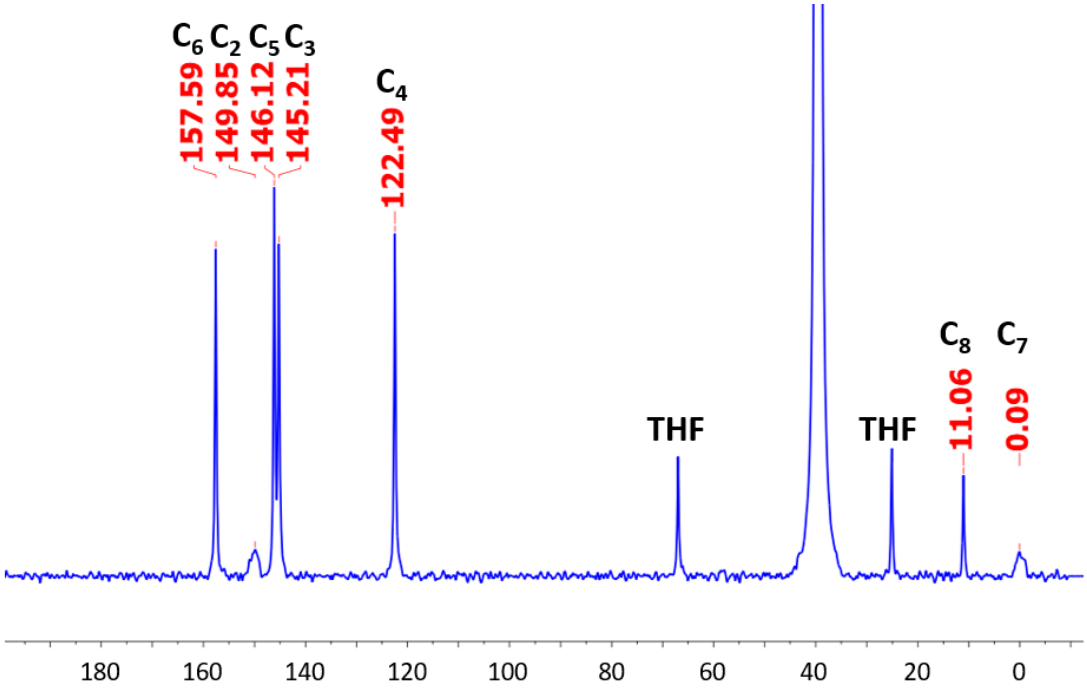

*Figure S3. $^{13}C\{^{1}H\}$ NMR (298 K, DMSO-d_6, 100.5 MHz) spectrum of **1**Li. Observation of signals at 149.85 (br, C_2) and -0.09 (br, C_7) ppm corresponding to Al–C bonded carbons was challenging due to their broadening, and a line broadening (lb) of 20 Hz was used in the processing of the spectrum. These signals were also detected through ^{1}H–^{13}C HMBC and ^{1}H–^{13}C HMQC experiments (see Fig S6 and S7).*

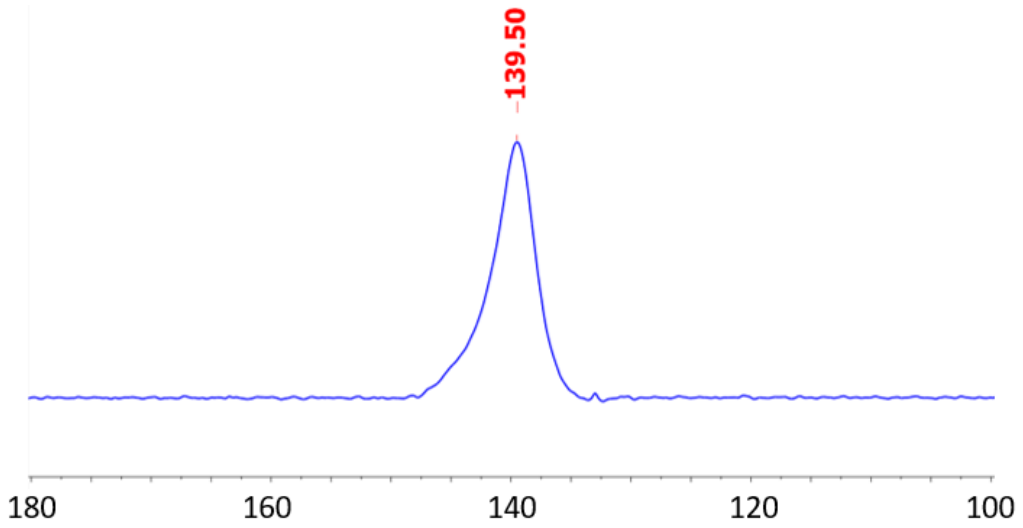

*Figure S4. ^{27}Al NMR (298 K, DMSO-d_6, 130.3 MHz) spectrum of **1**Li. Note: A line broadening (lb) of 50 Hz was used in the processing of the spectrum.*

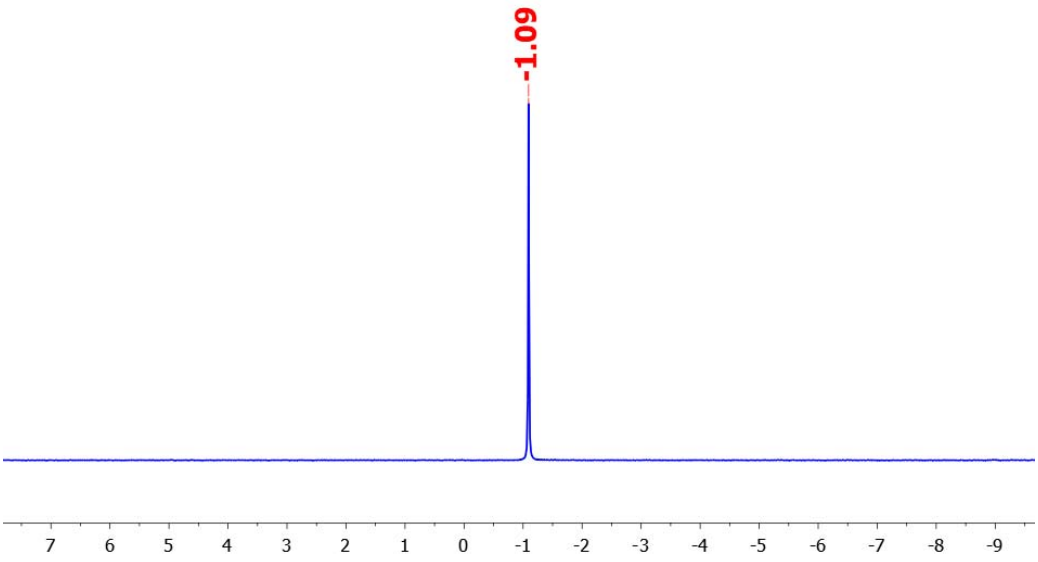

*Figure S5. ^{7}Li NMR (298 K, DMSO-d_6, 194.2 MHz) spectrum of **1**Li.*

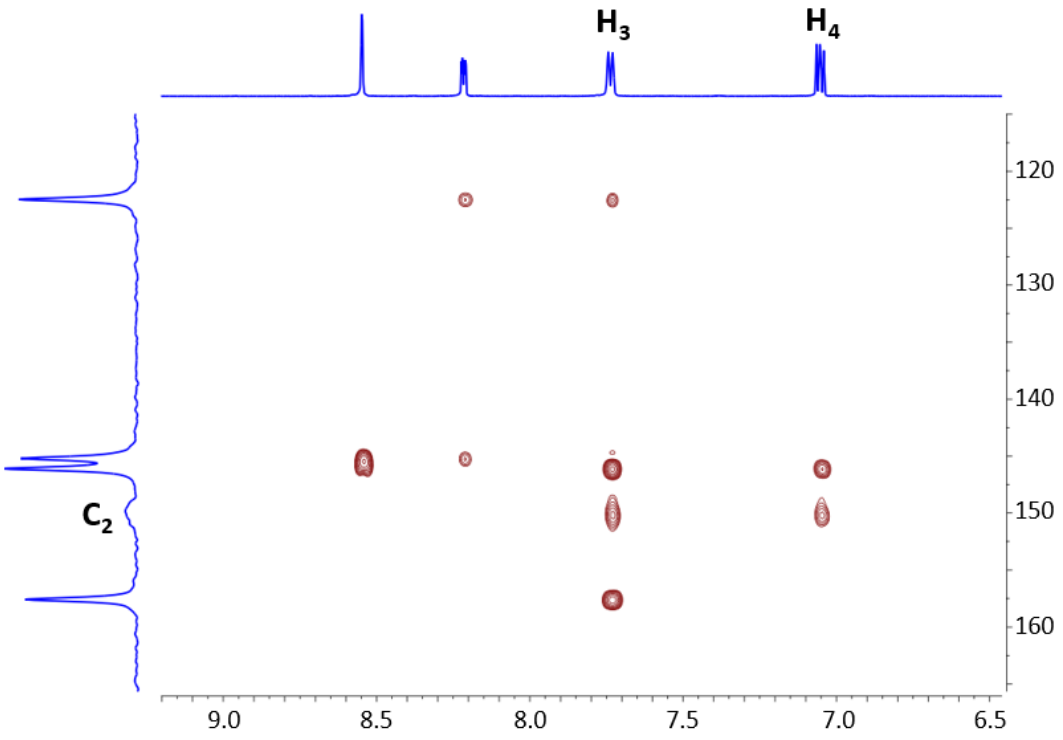

*Figure S6. Selected region of the ^{1}H–^{13}C HMBC (298 K, DMSO-d_6) spectrum of **1**Li used for the identification of the Al-bonded C_{py} (C_2) (broad signal at 149.85 ppm).*

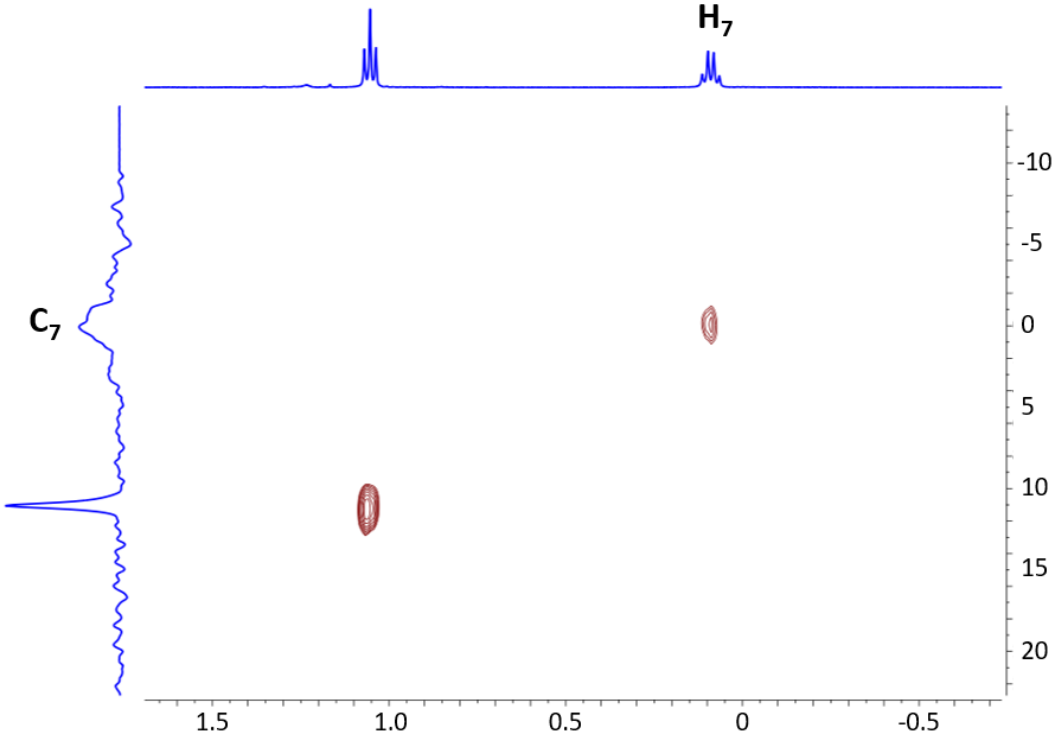

*Figure S7. Selected region of the $^{1}H–^{13}C$ HMQC (298 K, DMSO-d_6) spectrum of **1**Li used for the identification of the Al-bonded C_{Et} (C_7) (broad signal at -0.09 ppm).*

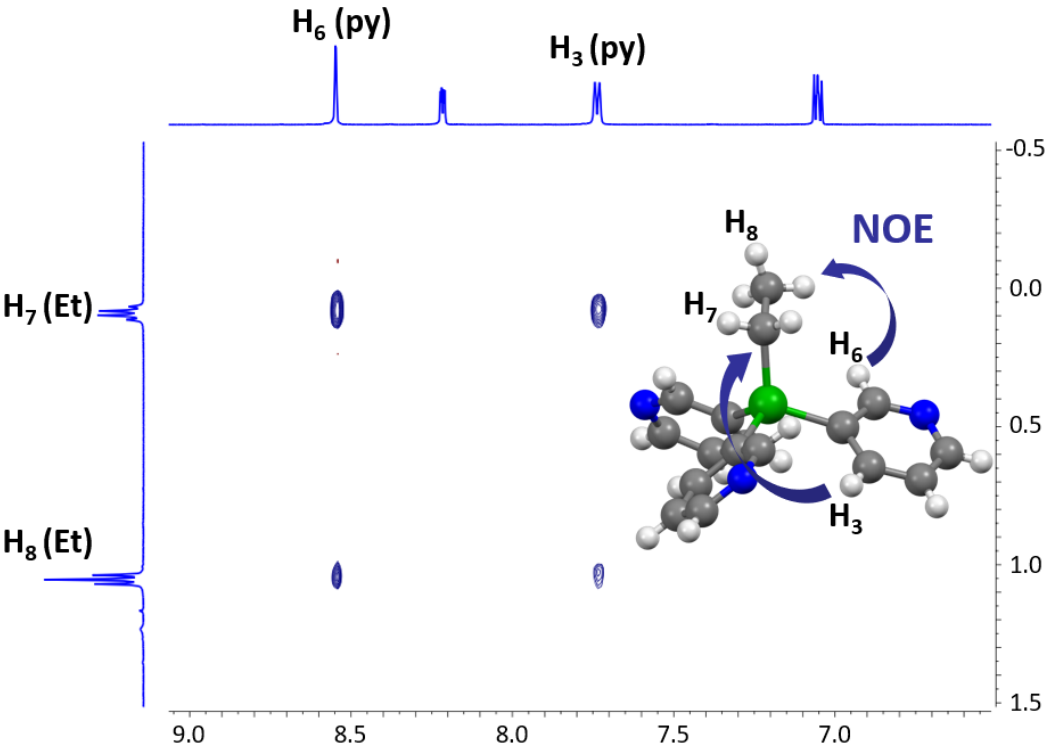

*Figure S8. Selected region of the $^{1}H–^{1}H$ NOESY (298 K, DMSO-d_6, mixing time of 800 ms) spectrum of **1**Li. Crosspeaks observed between the py-H_3 and py-H_6 protons of the pyridine and the protons of Al–CH_2–CH_3 arise from intramolecular cross-relaxation of protons that are close to each other in space, confirming the presence of an Et–Al–Py linkage.*

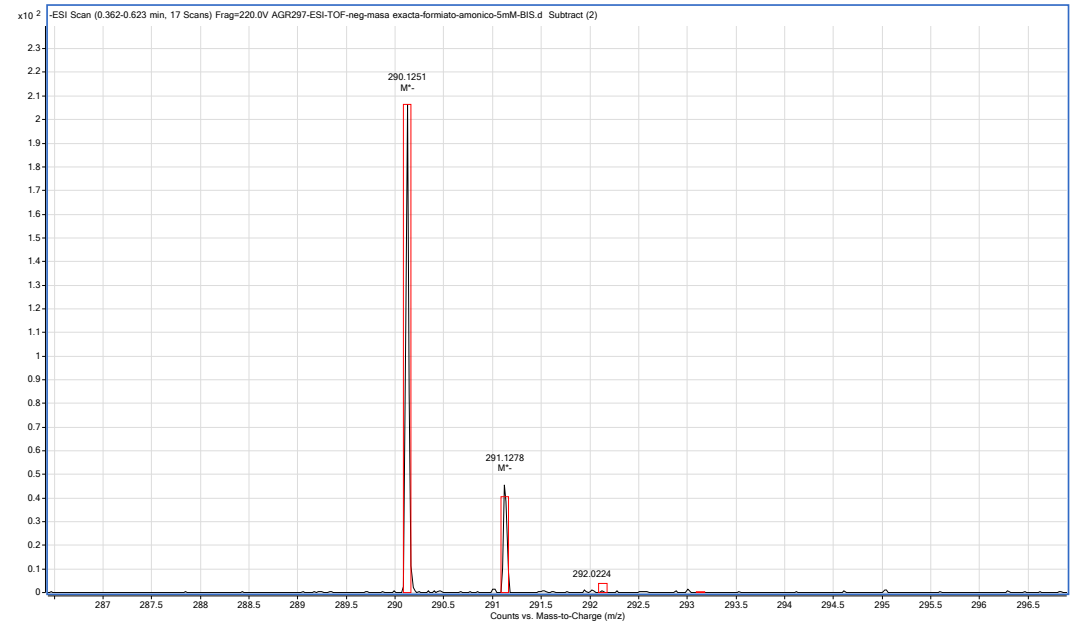

Best	Name	Formula	Score	Mass	Mass (Tgt)	Mass (DB)	Mass (MFG)	Diff (ppm)	Diff (abs. ppm)	Diff (mDa)
●		C17 H17 Al N3	81.58	290.1246			290.1238	-2.64	2.64	-0.76

Species	Ion Formula	m/z	Height	Score (MFG)	Score (MFG, MS)	Score (MFG, MS/MS)	Score (MFG, mass)	Score (MFG, abund)	Score (MFG, iso. spacing)
M*-	C17 H17 Al N3	290.1243	206.4	81.58	81.58		95.64	85.04	49.29

m/z	m/z (Calc)	Diff (ppm)	Diff (mDa)	Height	Height (Calc)	Height %	Height % (Calc)	Height Sum %	Height Sum% (Calc)
290.1251	290.1243	-2.65	-0.8	207	213	100	100	81.2	83.6
291.1278	291.1274	-1.48	-0.4	47.9	41.9	23.2	19.7	18.8	16.4

*Figure S9. HR-MS (ESI-TOF) (negative mode) of **1**Li showing the expected $[M]^-$ peak at m/z 290.1251 (calcd 290.1243; -2.65 ppm error).*

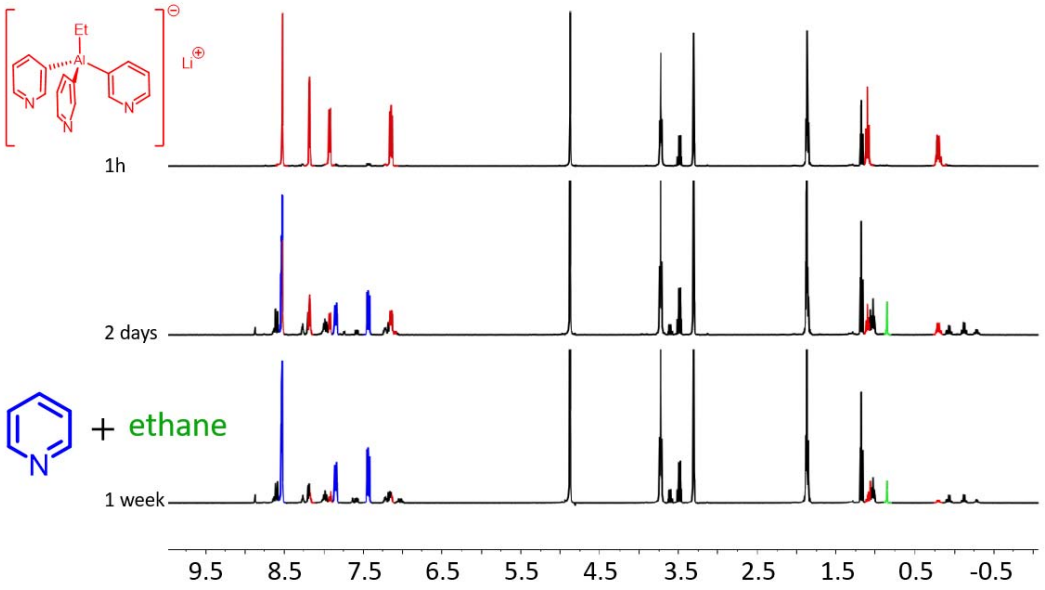

*Figure S10. Stacked ^{1}H NMR spectra of the evolution of a sample of **1**Li in CD_3OD over 1 h, 2 days and 1 week. No decomposition was observed after 1 h, and only prolonged storage in methanol led to its slow decomposition and the appearance of free pyridine (3-D-Py), along with small amounts of ethane and other unidentified species.*

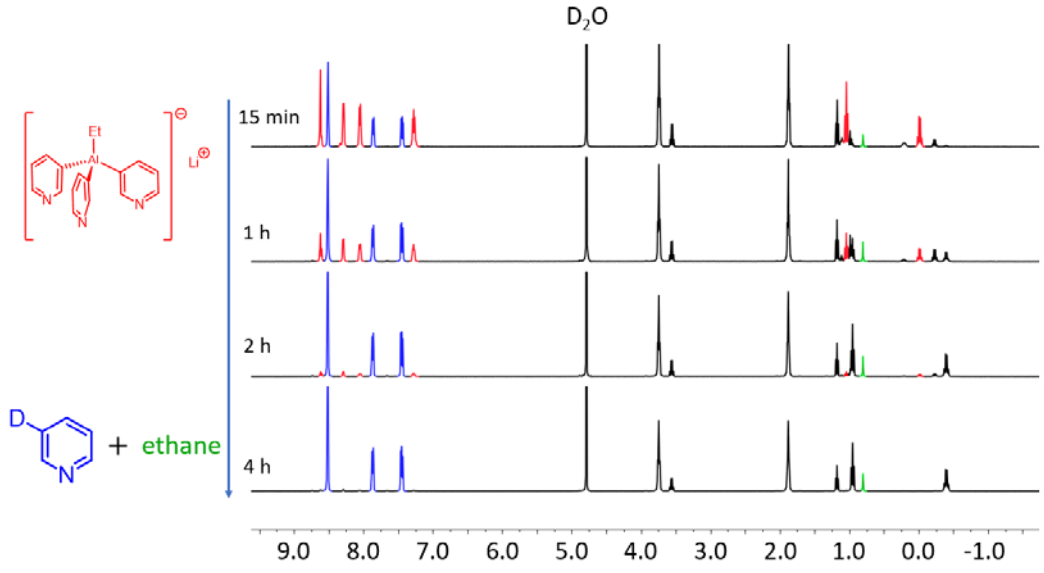

*Figure S11. Stacked ^{1}H NMR spectra of the evolution of a sample of **1**Li in D_2O over 15 min, 1 h, 2 h and 4 h. Partial decomposition to free pyridine (3-D-py), along with small amounts of ethane, was observed after 15 min.*

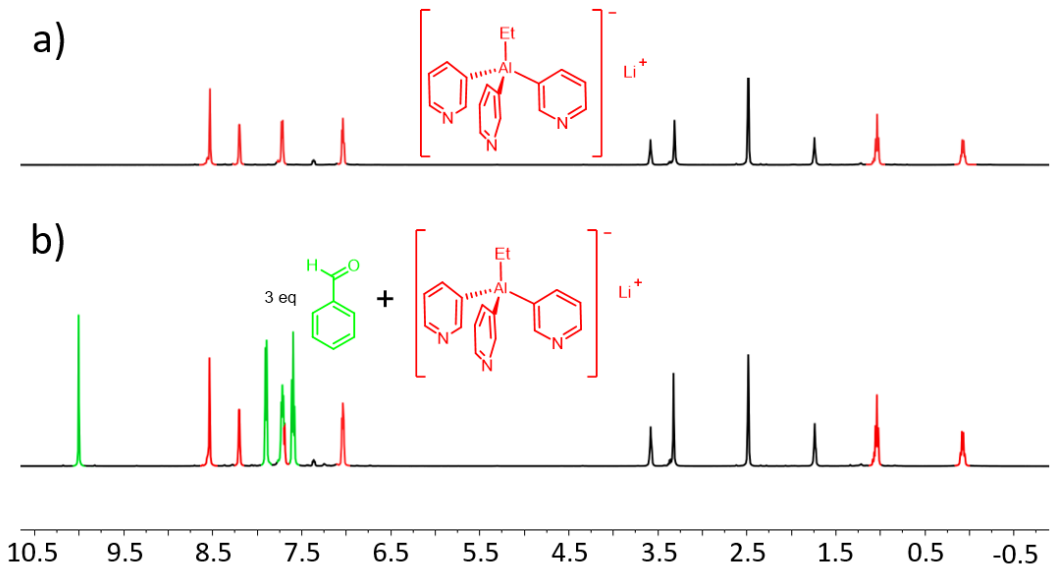

*Figure S12. a) ^{1}H NMR spectrum of **1**Li in DMSO-d_6. b) ^{1}H NMR spectrum of **1**Li in DMSO-d_6 after the addition of 3 eq of benzaldehyde. No evidence of nucleophilic addition to benzaldehyde or decomposition was observed after 5 days at room temperature.*

NMR studies and NMR spectra of 2Li

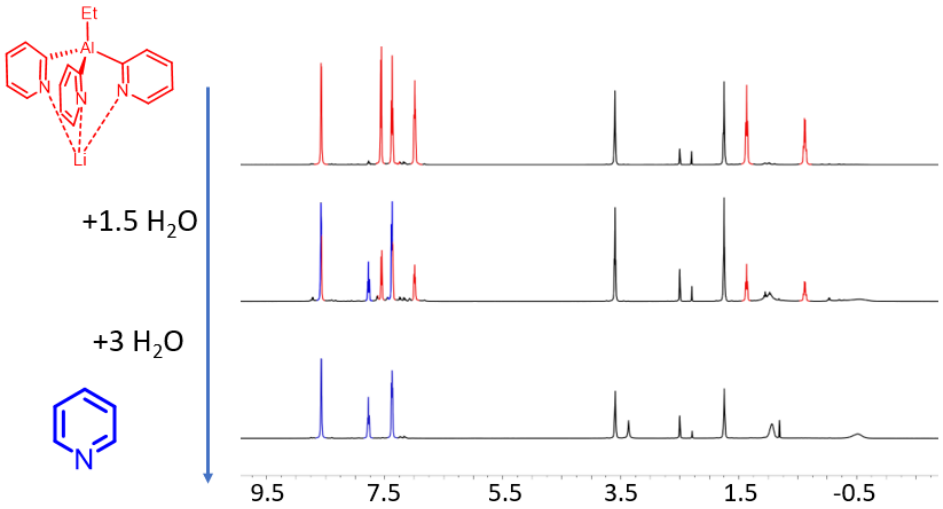

*Figure S13. Stacked ^{1}H NMR spectra of the successive addition of ca. 1.5 and 3 equiv of water to a solution of **2**Li in DMSO-d_6. As expected, **2**Li reacted immediately and quantitatively with H_2O in DMSO, leading to the formation of Py–H.*

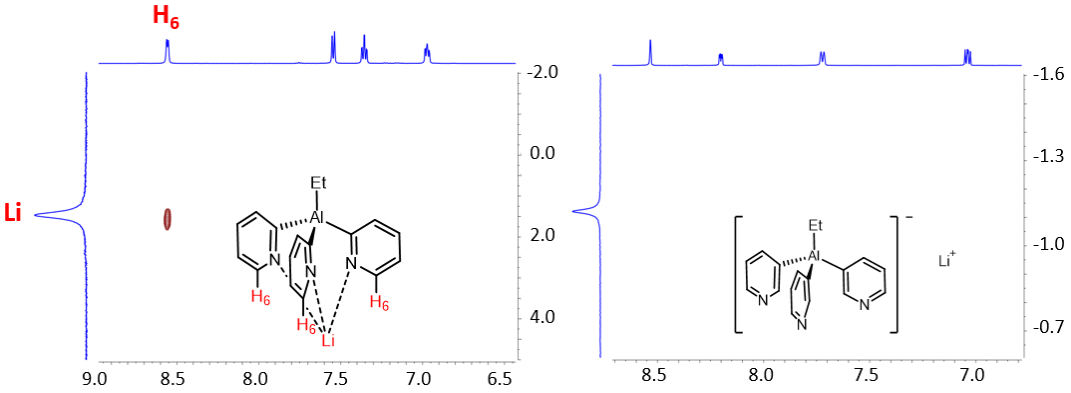

*Figure S14. Selected regions of the ^{1}H–^{7}Li HOESY NMR spectra of **1**Li (right) and **2**Li (left) in DMSO-d_6 at 298 K. The ^{1}H–^{7}Li HOESY NMR spectrum of **2**Li shows close spatial proximity between py-H_6 and Li, as expected for a CIP. Experiments under similar conditions for **1**Li did not provide any crosspeaks, and therefore no evidence for proximity between the Li and the aluminate framework, in agreement with a SIP.*

DOSY experiments

In order to evaluate whether **1**Li and **2**Li were likely to exist as a separated ion pair (SIP) or contact ion pair (CIP) in solution, we estimated its MW using ^{1}H and ^{7}Li DOSY. For **1**Li, the MW was first estimated using the internal calibration curve method with three standards,[1,2] and then using the Stalke method (ECC_{DMSO}^{DSE}, see pages S15–S17). As the determined MW (MW_{det}) values using both methods were similar, providing the same conclusions, and the Stalke method is more convenient to perform, this was the preferred method and was used for further experiments.

Estimation of the MW of 1Li using the DOSY-internal calibration curve (ICC)-MW method

In order to estimate the MW of **1**Li, we used an internal calibration curve using three internal standards. The determined MW (MW_{det}) was similar to the one obtained using the Stalke method (MW_{det} using ECC_{DMSO}^{DSE}), as shown in pages S15–S17.

^{1}H and ^{7}Li DOSY-ICC-MW estimation of **1**Li in DMSO-d_6 (27 mM) was conducted at 298 K. Tetraphenyl butadiene (TPB, MW 358.45), hexamethylbenzene (MW 162.27), and cyclohexene (MW 82.14) were used as internal references.

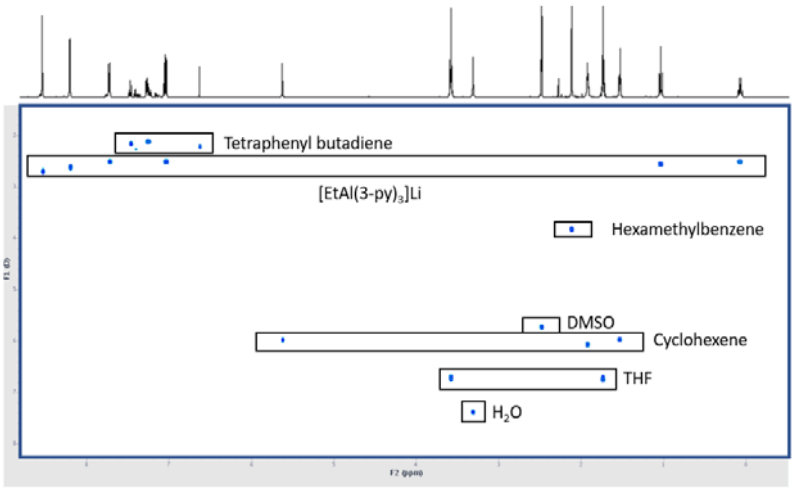

*Figure S15. ^{1}H DOSY NMR spectrum of **1**Li in DMSO-d_6 (27 mM) at 298 K in the presence of the inert standards hexamethylbenzene, cyclohexene and tetraphenyl butadiene (TPB).*

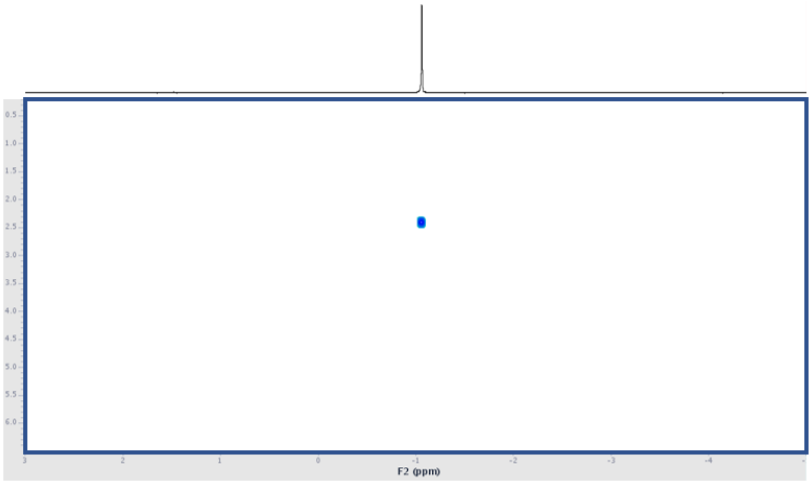

*Figure S16. ^{7}Li DOSY NMR spectrum of **1**Li in DMSO-d_6 (27 mM) at 298 K in the presence of the inert standards hexamethylbenzene, cyclohexene and tetraphenyl butadiene (TPB).*

Internal reference	D m²/S	logD	LogMW	Real MW
TPB	2.170E-10	-9.6634	2.5544	358.45
Hexamethylbenzene	3.819E-10	-9.4179	2.2102	162.27
Cyclohexene	6.002E-10	-9.2217	1.9145	82.14

*Table S1. LogD–LogMW analysis from the ^{1}H DOSY NMR data obtained for the mixture of **1**Li and the standards (hexamethylbenzene, cyclohexene and TPB) at 298 K in DMSO-d_6 in order to obtain an internal calibration line (y=-0.691x-7.896, R^2=0.9996).*

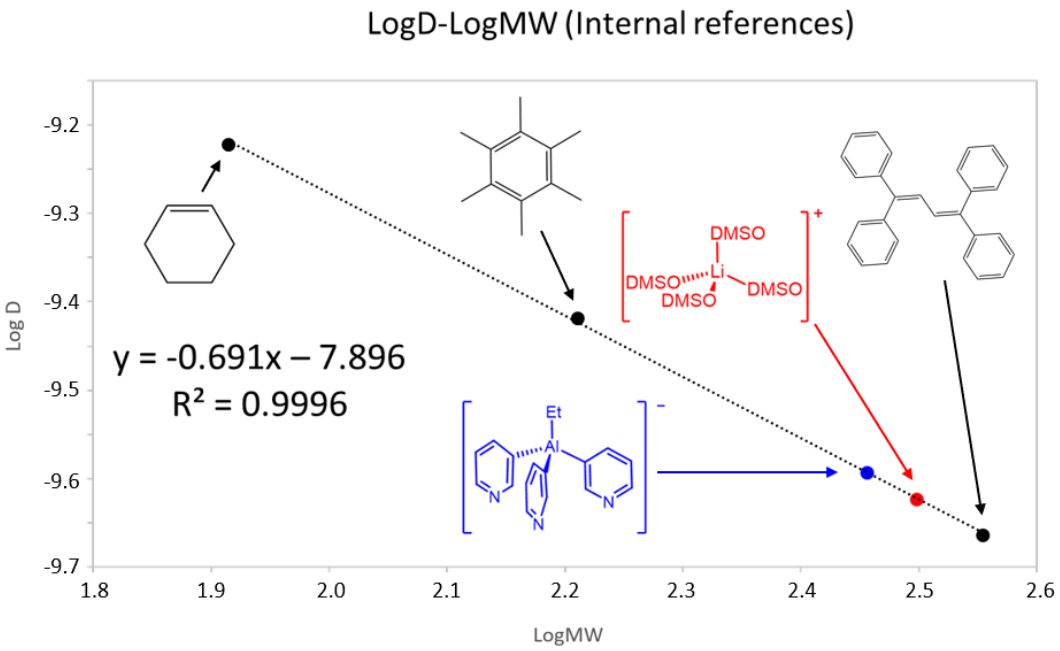

*Figure S17. LogD–LogMW plot prepared from the ^{1}H DOSY NMR (and ^{7}Li for $Li(DMSO)_4^+$) data obtained for the mixture of **1**Li and the standards hexamethylbenzene, cyclohexene and TPB at 298 K in DMSO-d_6. The MW determined for $EtAl(3\text{-}py)_3^-$ and $Li(DMSO)_4^+$ were 288 and 315, respectively.*

	D m^2/S	logD	LogMW	MW_{det}
1Li (^{1}H)	2.552E-10	-9.5929	2.4587	288
1Li (^{7}Li)	2.386E-10	-9.6223	2.4983	315

*Table S2. D–MW analysis from the ^{1}H and ^{7}Li DOSY NMR data obtained for the mixture of **1**Li and the standards hexamethylbenzene, cyclohexene and TPB at 298 K in DMSO-d_6.*

a)

Aggregate	MW_{det} (^{1}H-DOSY)	MW_{cal} (theoretical)	MW_{dif}[%]
$[EtAl(3\text{-}py)_3]^-$	288	290	1
$[EtAl(3\text{-}py)_3]Li{\cdot}DMSO$	288	375	31
$[EtAl(3\text{-}py)_3]Li{\cdot}(DMSO)_2$	288	454	58

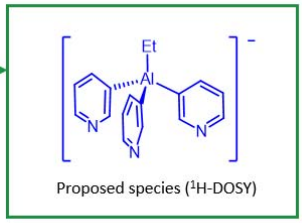

Proposed species (^{1}H-DOSY)

b)

Aggregate	MW_{det} (^{7}Li-DOSY)	MW_{cal} (theoretical)	MW_{dif}[%]
$[Li(DMSO)_2(THF)_2]^+$	315	307	-3
$[Li(DMSO)_4]^+$	315	319	2
$[Li_2(DMSO)_4(H_2O)_2]^{2+}$	315	362	15
$[EtAl(3\text{-}py)_3]Li{\cdot}DMSO$	315	375	20
$[EtAl(3\text{-}py)_3]Li{\cdot}(DMSO)_2$	315	454	45
$[Li_2(DMSO)_6]^{2+}$	315	483	54

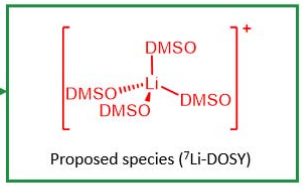

Proposed species (^{7}Li-DOSY)

*Figure S18. ICC was used to calculate the MW_{det} of **1**Li in DMSO-d_6 at 298 K and the MW_{dif} for the proposed species. MW_{det} extracted from (a) ^{1}H and (b) ^{7}Li-DOSY. Please note that the values listed in the main manuscript are those obtained using the Stalke method (see pages S15-S17).*

*Note 1: $[Li(DMSO)_2(THF)_2]^+$ (ref. 3) cannot be ruled out on the basis of its molecular weight, as DMSO and THF have similar molecular weights (78 and 72 g mol^{-1}, respectively). However the DOSY experiments show that THF diffuses as "free molecules" (THF MW real = 72 g mol^{-1}, MWdet = 70 g mol^{-1}) clearly indicating that the small amount of THF present (1 eqv) does not compete with the large excess of the highly coordinating solvent DMSO for Li coordination. $[Li(DMSO)_2(THF)_2]^{2+}$ (ref. 4) is also not very likely due to the small amount of H_2O present in the DOSY experiments concerning **1**Li (typically only 0.5–1 eqv of residual H_2O); additionally, in this case the MW difference is large enough to discount this species, as is the case for $[Li_2(DMSO)_6]^{2+}$ (ref. 5).*

Note 2: The deviation is calculated as $M_{dif} = [(MW_{cal}\text{-}MW_{det})/MW_{det}]\times100\%$ where MW_{det} is the experimentally determined value and MW_{cal} is the calculated molecular weight for the hypothetical species.

Estimation of the MW of 1Li using the DOSY-ECC$_{DSE}$-MW method (Stalke method)

We have found that the "Stalke method" using the ECC_{DMSO}^{DSE} (external calibration curve for dissipated spheres and ellipsoids in DMSO) was suitable to estimate the MW of pyridyl aluminate species in DMSO solution.[6,7,8] The conclusions obtained using this method parallel those obtained using ICC (*vide supra*).

^{1}H and ^{7}Li DOSY-ECC-MW estimation of **1**Li in DMSO-d$_6$ (54 mM) was carried out at 298 K. Adamantane was used as an internal reference with logD$_{ref,int}$ = -9.4157 (logD of the internal reference).

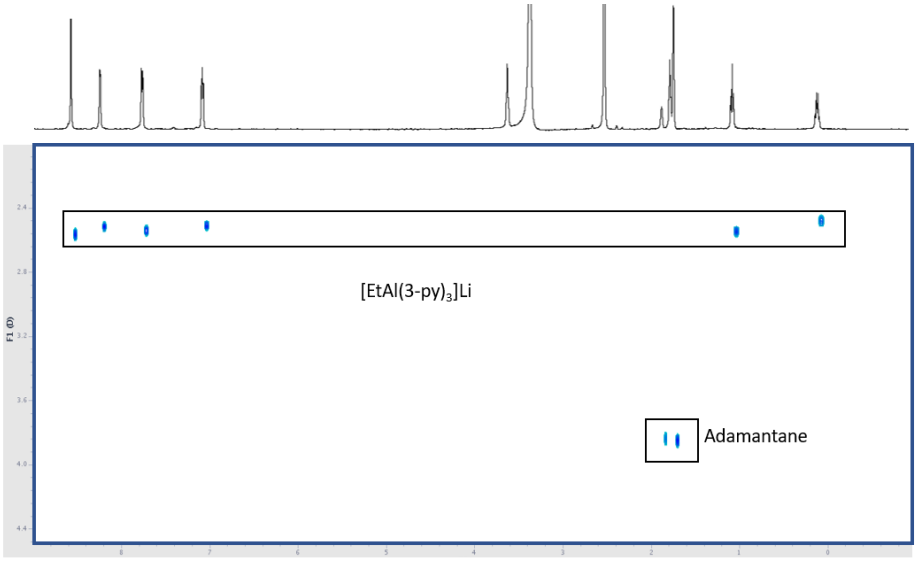

*Figure S19. ^{1}H DOSY NMR spectrum of **1**Li and adamantane (internal reference) at 298 K in DMSO-d$_6$.*

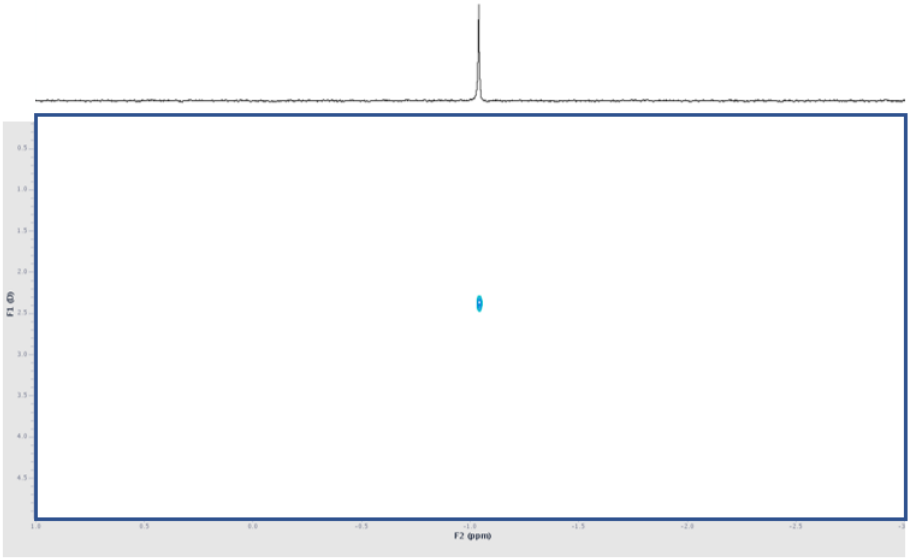

*Figure S20. ^{7}Li DOSY NMR spectrum of **1**Li and adamantane (internal reference) at 298 K in DMSO-d$_6$.*

Compound	D m²/s	log D	Log $D_{x,norm}$	MW (g/mol)
Adamantane	3.839E-10	-9.4157	-	136.23[a]
1Li (^{1}H)	2.520E-10	-9.5985	-9.5090	275[b]
1Li (^{7}Li)	2.370E-10	-9.6251	-9.5356	299[b]

*Table S3. D–MW analysis using the ^{1}H DOSY NMR data obtained for the mixture of **1**Li and adamantane (internal reference) at 298 K in DMSO-d_6. [a] Real MW. [b] MW_{det}.*

a)

Aggregate	MW_{det} (^{1}H-DOSY)	MW_{cal} (theoretical)	MW_{dif}[%]
$[EtAl(3\text{-}py)_3]^-$	275	290	6
$[EtAl(3\text{-}py)_3]Li{\cdot}DMSO$	275	375	37
$[EtAl(3\text{-}py)_3]Li{\cdot}(DMSO)_2$	275	454	65

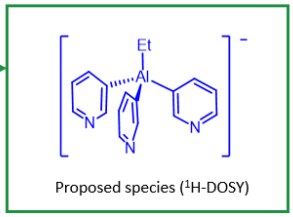

Proposed species (^{1}H-DOSY)

b)

Aggregate	MW_{det} (^{7}Li-DOSY)	MW_{cal} (theoretical)	MW_{dif}[%]
$[Li(DMSO)_2(THF)_2]^+$	299	307	3
$[Li(DMSO)_4]^+$	299	319	7
$[Li_2(DMSO)_4(H_2O)_2]^{2+}$	299	362	21
$[EtAl(3\text{-}py)_3]Li{\cdot}DMSO$	299	375	26
$[EtAl(3\text{-}py)_3]Li{\cdot}(DMSO)_2$	299	454	52
$[Li_2(DMSO)_6]^{2+}$	299	483	61

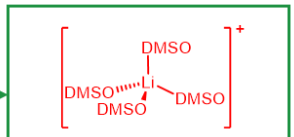

Proposed species (^{7}Li-DOSY)

*Figure S21. ECC_{DMSO}^{DSE} was used to determine the MW_{det} of **1**Li in DMSO-d_6 at 298 K and the MW_{dif} for the proposed species. MW_{det} extracted from (a) ^{1}H and (b) ^{7}Li-DOSY. Note: ECC_{DMSO}^{DSE} max. error = ± 8.*[7]

Note: $[Li(DMSO)_2(THF)_2]^+$ cannot be ruled out on the basis of its molecular weight. However the DOSY experiments show that THF diffuses as "free molecules" indicating that the small amount of THF present (1 eqv) does not compete with the large excess of the highly coordinating solvent DMSO for Li coordination. A similar argument should apply to rule out the species involving water, as there was typically only 0.5–1 eqv of residual H_2O in the DOSY experiments concerning 1Li; additionally, in this case the MW difference is large enough to discount this species (see also comments on Fig.S18).

The DOSY NMR data were analysed using the MW Estimation Software developed by Stalke.[8] The estimated molecular weight obtained using the ^{1}H NMR diffusion coefficient of **1**Li in DMSO-d_6 is 275 g mol^{-1}, which is just 6% lower than the expected value for a monomeric anion $[EtAl(3\text{-}py)_3]^-$ (290 g mol^{-1}). This difference is much greater for $[EtAl(3\text{-}py)_3]Li{\cdot}DMSO$ (37%) and $[EtAl(3\text{-}py)_3]Li{\cdot}(DMSO)_2$ (65%). The estimated molecular weight using the ^{7}Li NMR diffusion coefficient of **1**Li in DMSO-d_6 is 299 g mol^{-1}, which is just 7% lower than the expected value for $Li(DMSO)_4^+$. Although the molar van der Waals density (MD_w) of $Li(DMSO)_4^+$ is not within the range for a very precise molecular weight determination using the Stalke method, the molecular weight was nonetheless estimated for this species, and $[EtAl(3\text{-}py)_3]Li{\cdot}DMSO$ and $[EtAl(3\text{-}py)_3]Li{\cdot}(DMSO)_2$, which have molar van der Waals density that are suitable for very precise determination, have 26% and 52% higher MW_{dif} values, respectively. These data support the view that contact ion

pairs (CIPs) are not present in DMSO solution, indicating the coexistence of $[EtAl(3\text{-}py)_3]^-$ and $Li(DMSO)_4^+$ species.

Concentration	Compound	D m^2/s	log D	Log $D_{x,norm}$	MW (g/mol)
5.4 mM	Adamantane	4.004E-10	-9.3974	-	136.23[a]
	1Li (^{1}H)	2.587E-10	-9.5872	-9.5160	281[b]
81 mM	Adamantane	3.699E-10	-9.4318	-	136.23[a]
	1Li (^{1}H)	2.431E-10	-9.6140	-9.5084	274[b]

*Table S4. D–MW analysis from the ^{1}H DOSY NMR data obtained for the mixture of **1**Li and adamantane (internal reference) at 298 K in DMSO-d_6 at different concentrations (5.4×10^{-3} M and 8.1×10^{-2} M). [a] Real MW. [b] MW_{det}.*

Estimation of the MW of 2Li using the DOSY-ECC$_{DSE}$-MW method (Stalke method)

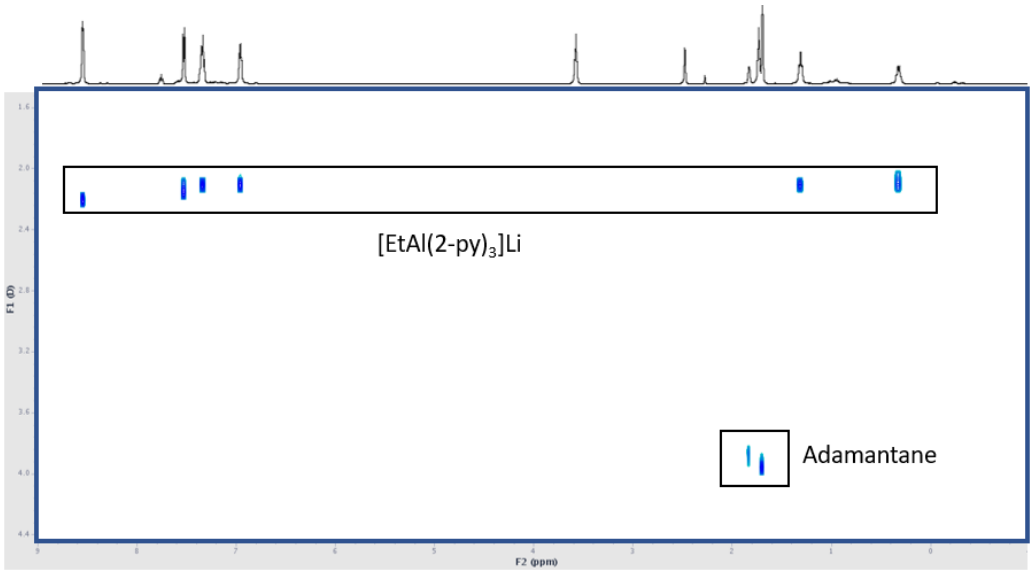

*Figure S22. ^{1}H DOSY NMR spectrum of **2**Li and adamantane (internal reference) at 298 K in DMSO-d_6.*

^{1}H DOSY-ECC-MW estimation of **2**Li in DMSO-d_6 (54 mM) was carried out at 298 K. Adamantane was used as an internal reference with $\log D_{ref,int}$ = -9.4039.

Compound	D m^2/s	log D	log D $_{x,norm}$	MW (g/mol)
Adamantane	3.944E-10	-9.4039	-	136.23[a]
2Li (^{1}H)	2.116E-10	-9.6744	-9.5967	365[b]

*Table S5. D-MW analysis from the ^{1}H DOSY NMR data obtained for the mixture of **2**Li and adamantane (internal reference) at 298 K in DMSO-d_6. [a] Real MW. [b] MW_{det}.*

Aggregate	MW_{det} (^{1}H-DOSY)	MW_{cal} (theoretical)	MW_{dif}[%]
$[EtAl(2\text{-}py)_3]^-$	365	290	-20
$[EtAl(2\text{-}py)_3]Li{\cdot}DMSO$	365	375	3
$[EtAl(2\text{-}py)_3]Li{\cdot}(DMSO)_2$	365	454	24

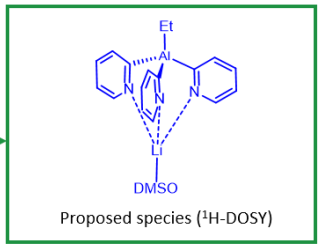

Proposed species (^{1}H-DOSY)

Figure S23. ECC_{DMSO}^{DSE} *was used to determine the* MW_{det} *of* ***2***Li *in DMSO-*d_6 *at 298 K and the* MW_{dif} *for the proposed species.* MW_{det} *extracted from* ^{1}*H-DOSY. Note:* ECC_{DMSO}^{DSE} *max. error = ± 8.*[7]

The estimated molecular weight using the proton diffusion coefficient of **2**Li in DMSO-d_6 is 365 g mol^{-1}, which is 3% lower than the anticipated value for the monomeric species $[EtAl(2\text{-}py)_3]Li{\cdot}DMSO$ (375 g mol^{-1}). The MW_{dif} values are much greater for $[EtAl(2\text{-}py)_3]^-$ (-20%) and $[EtAl(2\text{-}py)_3]Li{\cdot}(DMSO)_2$ (24%). These data support the view that a CIP is present in DMSO solution, indicating the existence of the species $[EtAl(2\text{-}py)_3]Li{\cdot}DMSO$.

Computational details

All computations were carried out using the Gaussian16 package,[9] in which the hybrid method of Austin, Petersson and Frisch with spherical atom dispersion terms (APFD) was applied.[10] The triple zeta 6-311+G(2d,p) basis set with polarization and diffuse functions was used for all the atoms. Geometry optimizations were performed without symmetry restrictions using the initial coordinates derived from X-ray data when available, and frequency analyses were performed to ensure that a minimum structure with no imaginary frequencies was achieved in each case. The visualization of the calculation results was performed with GaussView 6.1.[11]

$[EtAl(3\text{-}py)_3]^-$ (1) hydrolysis reaction thermochemistry

All the reactants and products of the hydrolysis reaction were optimized and the frequencies calculated in DMSO as the solvent using the SMD method.[12]

$$[EtAl(3\text{-}py)_3]^- + H_2O \rightarrow [EtAl(3\text{-}py)_2(OH)]^- + H\text{-}py.$$

Compound	G in DMSO (a.u.)
$[EtAl(3\text{-}py)_3]^-$	-1064.082889
H_2O	-76.390773
$[EtAl(3\text{-}py)_2(OH)]^-$	-892.437923
H-py	-248.082704

*Table S6. G (a.u.) values for reactants and products involved in the **2**Li hydrolysis. Please note that solvated Li^+ does not affect the thermodynamics since it is solvated on both sides of the equation.*

ΔG (hydrolysis) = -0.046965 a.u. = -29.5 kcal/mol

NBO atomic natural charges

The atomic charges resulting from natural population analysis were calculated using the program NBO 7.0 [13] for $[EtAl(3\text{-}py)_3]^-$ (**1**) and $[EtAl(2\text{-}py)_3]^-$ (**2**). The Al–C_{py} bond polarization, which was calculated as the difference in their atomic charges (see Figures S24 and S25), is shown in Table S7. In the case of chelating aluminate **1**, coordination to Li^+ does not substantially affect the Al–C bond polarity (Figure S26).

NBO analyses were also carried out for the methyl analogues of aluminates **1** and **2**, which are shown in Table S8 and Figures S27–S29, leading to the same conclusions.

Compound	$\Delta\delta$ Al-C_{py}
$[EtAl(3\text{-}py)_3]^-$	2.067
$[EtAl(2\text{-}py)_3]^-$	1.717
$[EtAl(2\text{-}py)_3]Li{\cdot}THF$	1.587

Table S7. The Al–C_{py} bond polarization, calculated as the difference in their atomic charges.

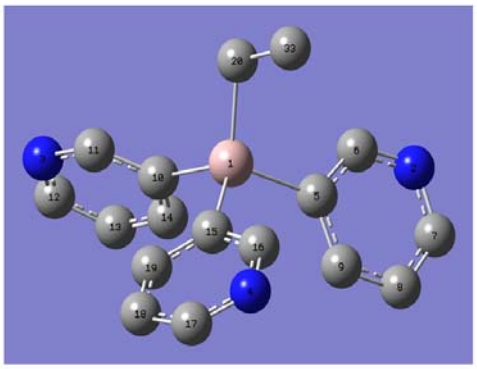

Atom	NBO atomic charge
Al1	+1.540
C20	-0.972
C5	-0.527
C6	+0.047
N2	-0.490
C7	+0.019
C8	-0.272
C9	-0.176

Figure S24. $[EtAl(3\text{-}py)_3]^-$ with H atoms omitted for clarity. The atomic charges are listed in the table, with the values for the atoms in the pyridinic rings averaged over the three rings.

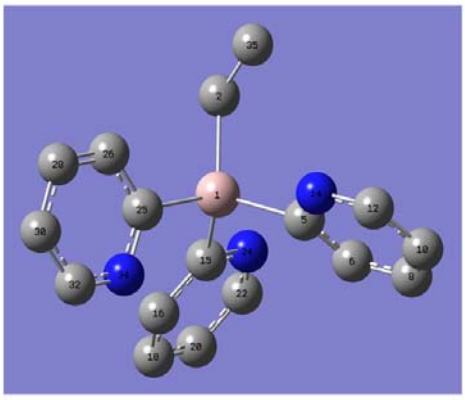

Atom	NBO atomic charge
Al1	+1.504
C2	-0.974
C5	-0.213
C6	-0.247
C8	-0.199
C10	-0.287
C12	+0.031
N14	-0.493

Figure S25. $[EtAl(2\text{-}py)_3]^-$ with H atoms omitted for clarity. The atomic charges are listed in the table, with the values for the atoms in the pyridinic rings averaged over the three rings.

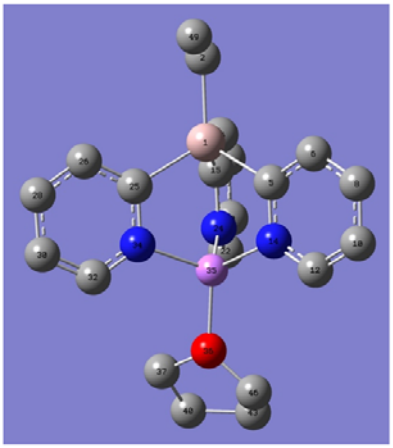

Atom	NBO atomic charge
Al1	+1.400
C2	-0.977
C5	-0.187
C6	-0.239
C8	-0.176
C10	-0.267
C12	+0.035
N14	-0.533

Figure S26. $[EtAl(2\text{-}py)_3]Li\cdot THF$ with H atoms omitted for clarity. The atomic charges are listed in the table, with the values for the atoms in the pyridinic rings averaged over the three rings.

- *Me derivatives*

As in the case of **1** and **2**, the Al–C_{3py} bond is more polarized than the Al–C_{2py} bond for the corresponding Me derivatives, and the coordination of Li in the chelating $[MeAl(2\text{-}Py)_3]^-$ does not change the bond polarity substantially (Table S8).

Compound	$\Delta\delta$ Al-C_{py}
$[MeAl(3\text{-}py)_3]^-$	2.037
$[MeAl(2\text{-}py)_3]^-$	1.696
$[MeAl(2\text{-}py)_3]Li{\cdot}THF$	1.646

Table S8. The Al–C_{py} bond polarization, calculated as the difference in their atomic charges (see Figures S27, S28 and S29).

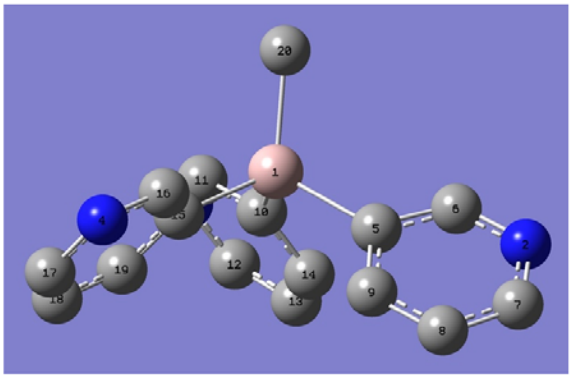

Atom	NBO atomic charge
Al1	+1.513
C20	-1.215
C5	-0.524
C6	+0.049
N2	-0.491
C7	+0.018
C8	-0.272
C9	-0.177

Figure S27. $[MeAl(3\text{-}py)_3]^-$ with H atoms omitted for clarity. The atomic charges are listed in the table, with the values for the atoms in the pyridinic rings averaged over the three rings.

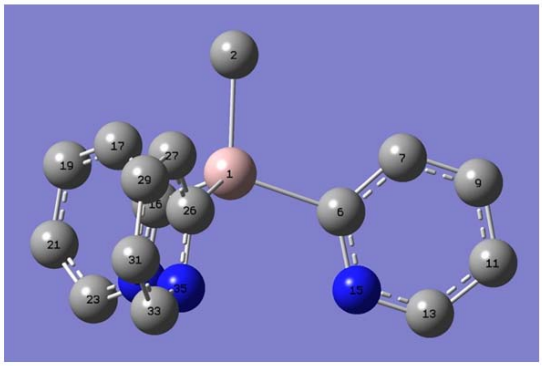

Atom	NBO atomic charge
Al1	+1.485
C2	-1.238
C6	-0.211
C7	-0.258
C9	-0.202
C11	-0.287
C13	+0.035
N15	-0.463

Figure S28. $[MeAl(2\text{-}py)_3]^-$ with H atoms omitted for clarity. The atomic charges are listed in the table, with the values for the atoms in the pyridinic rings averaged over the three rings.

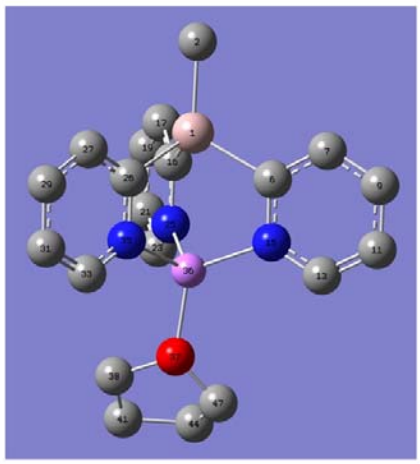

Atom	NBO atomic charge
Al1	+1.447
C2	-1.232
C6	-0.199
C7	-0.237
C9	-0.173
C11	-0.265
C13	+0.047
N15	-0.575

Figure S29. [MeAl(2-py)$_3$]Li·THF with H atoms omitted for clarity. The atomic charges are listed in the table, with the values for the atoms in the pyridinic rings averaged over the three rings.

A possible reaction pathway for the hydrolysis of [MeAl(2-py)$_3$]Li in DMSO modelled by DFT.

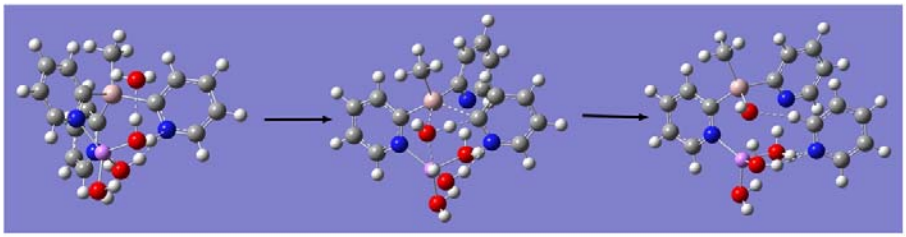

	[MeAl(2-py)$_3$]Li·(H$_2$O)$_3$	TS	[MeAl(2-py)$_2$(OH)]Li·(H$_2$O)$_3$ + H-py
	1	2	3
G (a.u.)	-1337.563353	-1337.533136	-1337.612296

Figure S30. Steps of the hydrolysis mechanism of [MeAl(2-py)$_3$]Li in DMSO.

Compound	G in DMSO (a.u.)
1	-1337.563353
2	-1337.533136
3	-1337.612296

Table S9. G (a.u.) values for compounds 1, 2 and 3.

ΔG = -0.048943 a.u. = -30.7 kcal/mol

$\Delta G^{\#}$ = 0.030217 a.u. = 19.0 kcal/mol

Cartesian coordinates

1 G (a.u.) = -1337.563353

Al	-0.48897400	-0.25986100	-1.12216500
C	-0.72823300	-0.51061200	-3.09086000
H	0.20169800	-0.40723700	-3.66753600
H	-1.42813000	0.22337100	-3.51250900
H	-1.13596700	-1.49966000	-3.33887200
C	0.23407800	1.64120400	-0.87290300
C	0.41533100	2.43223400	-2.02446800
H	1.05841500	3.86329300	1.42743500
C	0.83355200	3.75959900	-1.94055500
H	1.38660900	5.33754900	-0.55772600
C	1.06498200	4.30829200	-0.68477700
H	0.97218500	4.35566600	-2.84002900
C	0.87910000	3.48526800	0.42125300
H	0.21656100	1.99247100	-2.99829200
N	0.49035000	2.20846700	0.33952700
C	0.81371700	-1.74074900	-0.52118700
C	1.33054000	-2.57516200	-1.53216300
H	1.07221200	-2.36525500	-2.56663000
C	2.14654400	-3.66618600	-1.23749500
H	2.54044700	-4.29434300	-2.03354900
C	2.43931400	-3.94344000	0.09295000
H	3.06062100	-4.78571400	0.38164700
C	1.91120900	-3.09166700	1.05597900
H	2.11735200	-3.25564500	2.11287100
N	1.14723700	-2.03092300	0.77013500
C	-2.31064400	-0.40993100	-0.23261600
C	-3.44712500	-0.56491400	-1.04722900
H	-3.31729800	-0.63640800	-2.12412200
C	-4.72570200	-0.62717700	-0.50121900
H	-5.59756000	-0.74612400	-1.14111300
C	-4.87009500	-0.53480600	0.87981900
H	-5.84422100	-0.57687500	1.35810100
C	-3.71607500	-0.38955900	1.64037700
H	-3.76858300	-0.31983700	2.72586900
N	-2.49222100	-0.32781300	1.11013800
Li	0.81158100	1.12924200	1.93987300
O	1.13093500	1.66626800	3.79480900
H	0.56741800	0.89560200	3.97135700
H	2.02489800	1.30104800	3.75565700
O	-0.24605800	-0.32378500	2.45116200
H	0.19690200	-1.07840100	1.99725300
H	-1.16765600	-0.29261400	2.01726800
O	2.53711600	0.30629600	1.70616300
H	2.16950800	-0.58540300	1.56893900
H	2.90861400	0.51493400	0.82134300
O	3.16808300	0.50328600	-0.95842200
H	2.49721200	1.11569400	-1.29101200

H	2.82955200	-0.36465300	-1.21556300

2 G (a.u.) = -1337.533136

Al	0.18363700	0.56253400	-1.22496300
C	-0.07750600	1.62487500	-2.88753000
H	0.73214500	1.43066500	-3.60454300
H	-0.06341600	2.70665600	-2.70523000
H	-1.01572000	1.41567300	-3.41798800
C	2.11358600	0.51660100	-0.60744200
C	2.91906100	1.62423700	-0.92833900
H	4.31746600	-1.29542500	1.04759900
C	4.25352100	1.68635900	-0.54134500
H	5.82301700	0.62016100	0.51399900
C	4.78881000	0.62479500	0.18277000
H	4.86818500	2.54692500	-0.79762500
C	3.95041700	-0.44325700	0.47654900
H	2.48343700	2.44564500	-1.49427800
N	2.66738600	-0.50517900	0.09748500
C	-1.77643100	-0.87199100	-1.06186700
C	-2.94885600	-0.20596700	-1.45579900
H	-2.87776000	0.59404400	-2.18861300
C	-4.18310600	-0.53764500	-0.91084000
H	-5.08599300	-0.01226600	-1.21452300
C	-4.24552800	-1.55969800	0.03450100
H	-5.18418500	-1.85849300	0.49135100
C	-3.06142400	-2.19779900	0.37935000
H	-3.05902100	-3.00597900	1.10934200
N	-1.87168700	-1.87584200	-0.14499500
C	-0.70634900	1.55676200	0.33053500
C	-1.43667100	2.73527600	0.09293700
H	-1.57055300	3.07481000	-0.93123600
C	-1.98726500	3.46769800	1.13888600
H	-2.54739000	4.38016100	0.94414100
C	-1.80989900	3.01325900	2.44347200
H	-2.21866200	3.54659100	3.29657500
C	-1.09155300	1.83840500	2.62322400
H	-0.93232600	1.42821500	3.61945300
N	-0.55898900	1.14341000	1.61379700
Li	1.56210500	-1.97592600	0.77140200
O	2.10214200	-3.13475700	2.24827800
H	1.32301200	-2.69721300	2.63571200
H	1.77179800	-3.97332100	1.90604800
O	0.11168800	-1.36216500	1.84204100
H	-0.65199200	-1.67284100	1.32077700
H	-0.03660600	-0.34879200	1.85125400
O	0.64433700	-3.16715100	-0.40095200
H	-0.30106100	-2.92618500	-0.26336600
H	0.82802100	-2.76467800	-1.27004700
O	0.45741600	-1.25763300	-2.29808800
H	-0.60075700	-1.15481600	-1.94876200
H	0.53828700	-1.05923800	-3.23833600

3 G (a.u.) = -1337.612296

Al	1.12286000	1.35356700	-1.03617000
C	1.63123500	3.07400500	-1.89015700
H	2.46972000	2.95943900	-2.58944100
H	1.94523100	3.82418700	-1.15197900
H	0.80983300	3.52828100	-2.46047700
C	2.71034400	0.46307900	-0.15901500
C	3.83799200	1.22928400	0.18395400
H	3.72238900	-2.49673500	0.88555600
C	4.94844800	0.65352600	0.79296200
H	5.76467100	-1.21619000	1.53323400
C	4.92752600	-0.71198800	1.05919900
H	5.81623500	1.25571500	1.05468700
C	3.79188100	-1.42687900	0.69634600
H	3.83516500	2.29403500	-0.04003700
N	2.72317200	-0.87168000	0.10911900
C	-2.50424300	-0.45731000	-1.11315500
C	-3.57658100	0.38735500	-0.83960500
H	-3.52460600	1.43121000	-1.13044800
C	-4.67807500	-0.12658500	-0.16472400
H	-5.52687000	0.50845400	0.07519200
C	-4.67409700	-1.47090500	0.20242300
H	-5.51275200	-1.91712500	0.72807300
C	-3.55702800	-2.23702100	-0.11114900
H	-3.50822700	-3.28773400	0.16750900
N	-2.48674000	-1.74869700	-0.75065500
C	-0.35241800	1.66408000	0.33201500
C	-1.05793100	2.88180700	0.32015500
H	-0.77937600	3.63793500	-0.41058200
C	-2.09298100	3.13270800	1.21589300
H	-2.63190000	4.07794500	1.19382900
C	-2.42589700	2.15049500	2.14480200
H	-3.22423000	2.29180900	2.86751900
C	-1.69445800	0.96964500	2.12295600
H	-1.91411500	0.16484200	2.82335400
N	-0.70137900	0.73460500	1.26038800
Li	1.21879800	-2.12891500	-0.20922800
O	1.57874100	-3.79767900	0.78076000
H	0.88705400	-3.39040200	1.33419400
H	1.14996600	-4.52546900	0.31962800
O	-0.18869800	-1.82592200	1.09899100
H	-0.97677400	-1.99221200	0.55730700
H	-0.24106200	-0.81485900	1.24247500
O	0.23177000	-2.33855400	-1.79675700
H	-0.71607900	-2.40500900	-1.58975000
H	0.33764000	-1.39336100	-2.10685400
O	0.42683800	0.21611700	-2.26989500
H	-1.61643900	-0.09068400	-1.62670600
H	0.64406600	0.46324000	-3.17254200

X-Ray Crystallographic Studies

Diffraction data were collected using an Oxford Diffraction Supernova diffractometer equipped with an Atlas CCD area detector and a four-circle kappa goniometer. For the data collection, Mo or Cu micro-focused sources with multilayer optics were used. When necessary, crystals were mounted directly from solution using perfluorohydrocarbon oil to prevent atmospheric oxidation, hydrolysis, and solvent loss. Data integration, scaling, and empirical absorption correction were performed using the CrysAlisPro software package. The structure was solved by direct methods and refined by full-matrix-least-squares against F^2 with SHELX in OLEX2. Non-hydrogen atoms were refined anisotropically, and hydrogen atoms were placed at idealized positions and refined using the riding model. Graphics were made using OLEX2 and MERCURY.

The framework structure of compound **1**Li is clear with one well-resolved THF molecule coordinated to lithium. The structure contains additional void space with another poorly defined molecule of THF. Attempts to model this molecule of THF failed, and an therefore Olex2 solvent mask was applied. A solvent mask was calculated and 86 electrons were found in a volume of 376 cubic angstroms in 1 void per unit cell. The crystallization solvent was THF/toluene and this is consistent with the presence of two THF molecules per unit cell (i.e., one molecule of THF per unit formula) which account for 80 electrons per unit cell, and is also consistent with the NMR data of freshly prepared crystals. Further details of the data collections and structural refinements are given in Table S10.

*Table S10. Selected bond length and angles of **1**LiTHF.*

	1Li
Al-C_{Et}	1.981(3)
Al-C_{py}	2.009(3)-2.016(3)
Li-N	2.026(5)-2.037(6)
Li-O_{THF}	1.940(5)
C_{py}-Al-C_{py}	107.6(1)-108.7(1)
C_{py}-Al-C_{Et}	109.8(2)-112.6(2)
N-Li-N	109.3(2)-110.9(2)
N-Li-O_{THF}	108.5(2)-109.0(2)

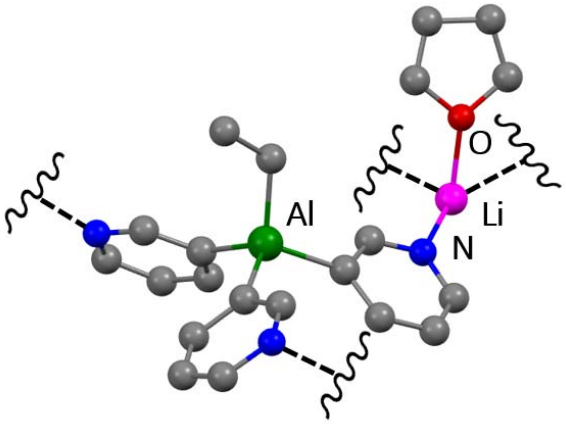

Table S11. Crystallographic data.

CCDC	2095751
	1Li·THF
Empirical formula	$C_{21}H_{25}AlLiN_3O$
Formula weight	369.36
Temperature/K	220.0(4)
Crystal system	triclinic
Space group	P-1
a/Å	10.0339(8)
b/Å	10.0431(6)
c/Å	15.9941(12)
α/°	81.015(6)
β/°	76.374(7)
γ/°	60.358(7)
V [Å^3]	1359.90(19)
Z	2
ρ_{calc}g/cm^3	0.902
μ/mm^{-1}	0.728
F(000)	392.0
Crystal size [mm]	0.47 × 0.28 × 0.14
Radiation	Cu Kα (λ = 1.54184)
2Θ range for data collection[°]	10.146 to 133.192
Index ranges	$-11 \leq h \leq 7$, $-11 \leq k \leq 10$, $-19 \leq l \leq 18$
Reflns collected	8565
Ind. Refl. [R(int)]	4778 [R_{int} = 0.0224, R_{sigma} = 0.0316]
Data/restraints/parameters	4778/44/256
GOF on F^2	1.050
Final R indexes [I>=2σ (I)]	R_1 = 0.0709, wR_2 = 0.2208
Final R indexes [all data]	R_1 = 0.0847, wR_2 = 0.2392
Max/min Δρ [eÅ^{-3}]	0.46/-0.30

References

1 D. Li, I. Keresztes, R. Hopson and P. G. Williard, *Acc. Chem. Res.*, 2009, **42**, 270–280.

2 D. Li, G. Kagan, R. Hopson and P. G. Williard, *J. Am. Chem. Soc.*, 2009, **131**, 5627–5634.

3 S. Bieller, M. Bolte, H.-W. Lerner and M. Wagner, *J.Organomet.Chem.* 2005, **690**, 1935-1946.

4 J. M. Butler and G. M. Gray, *J. Chem.Cryst.*, 2003, **33**, 557-562.

5 L. Liu, L. N. Zakharov, J. A. Golen, A. L. Rheingold and T. A. Hanna, *Inorg.Chem.*, 2008, **47**, 11143-11153.

6 R. Neufeld and D. Stalke, *Chem. Sci.*, 2015, **6**, 3354–3364.

7 S. Bachmann, R. Neufeld, M. Dzemski and D. Stalke, *Chem. – Eur. J.*, 2016, **22**, 8462–8465.

8 S. Bachmann, B. Gernert and D. Stalke, *Chem. Commun.*, 2016, **52**, 12861–12864. (The software is available for download at: http://www.stalke.chemie.uni-goettingen.de/mwestimation/)

9 Gaussian 16, Revision C.01, M. J. Frisch, G. W. Trucks, H. B. Schlegel, G. E. Scuseria, M. A. Robb, J. R. Cheeseman, G. Scalmani, V. Barone, G. A. Petersson, H. Nakatsuji, X. Li, M. Caricato, A. V. Marenich, J. Bloino, B. G. Janesko, R. Gomperts, B. Mennucci, H. P. Hratchian, J. V. Ortiz, A. F. Izmaylov, J. L. Sonnenberg, D. Williams-Young, F. Ding, F. Lipparini, F. Egidi, J. Goings, B. Peng, A. Petrone, T. Henderson, D. Ranasinghe, V. G. Zakrzewski, J. Gao, N. Rega, G. Zheng, W. Liang, M. Hada, M. Ehara, K. Toyota, R. Fukuda, J. Hasegawa, M. Ishida, T. Nakajima, Y. Honda, O. Kitao, H. Nakai, T. Vreven, K. Throssell, J. A. Montgomery, Jr., J. E. Peralta, F. Ogliaro, M. J. Bearpark, J. J. Heyd, E. N. Brothers, K. N. Kudin, V. N. Staroverov, T. A. Keith, R. Kobayashi, J. Normand, K. Raghavachari, A. P. Rendell, J. C. Burant, S. S. Iyengar, J. Tomasi, M. Cossi, J. M. Millam, M. Klene, C. Adamo, R. Cammi, J. W. Ochterski, R. L. Martin, K. Morokuma, O. Farkas, J. B. Foresman and D. J. Fox, Gaussian, Inc., Wallingford CT, 2019.

10 A. Austin, G. A. Petersson, M. J. Frisch, F. J. Dobek, G. Scalmani and K. Throssell, *J. Chem Theory Comput*., 2012, **8**, 4989–5007.

11 GaussView, Version 6.1, Roy Dennington, Todd A. Keith and John M. Millam, Semichem Inc., Shawnee Mission, KS, 2016.

12 A. V Marenich, C. J. Cramer and D. G. Truhlar, *J. Phys. Chem. B*, 2009, **113**, 6378–6396.

13 NBO 7.0. E. D. Glendening, J. K. Badenhoop, A. E. Reed, J. E. Carpenter, J. A. Bohmann, C. M. Morales, P. Karafiloglou, C. R. Landis and F. Weinhold, Theoretical Chemistry Institute, University of Wisconsin, Madison, WI (2018)